NEOPLASMA accepted, ahead of print manuscript
Cite article as https://doi.org/10.4149/neo_2021_210305N285

Running title: Effect of circSEC24A on the progression of HCC

CircSEC24A promotes tumor progression through sequestering miR-455-3p in hepatocellular carcinoma

Yulin Liao[1], Dongming Yang[2], Huaichao Luo[1], Guishu Yang[3], Xiaoxia Wen[4], Kaijiong Zhang[1], Chang Liu[1], Ruiling Zu[1], Lichun Wu[1], Zuo Wang[1], Dongsheng Wang[1,*]

[1]Department of Clinical Laboratory, Sichuan Cancer Hospital and Institute, Sichuan Cancer Center, School of Medicine, University of Electronic Science and Technology of China, Chengdu, Sichuan, China; [2]Department of Clinical Laboratory, The Fifth Affiliated Hospital of Sun Yat-sen University, Zhuhai, Guangdong, China; [3]College of Clinical Medicine, Southwest Medical University, Luzhou, Sichuan, China; [4]Clinical College, Chengdu University of Traditional Chinese Medicine, Chengdu, Sichuan, China

*Correspondence: dswang08@163.com

Received March 5, 2021 / Accepted May 27, 2021

Hepatocellular carcinoma (HCC) ranks third in the cause of death due to cancer. Circular RNA circSEC24 Homolog A (circSEC24A) has been uncovered to be upregulated in liver cancer. However, the function of circSEC24A in HCC is indistinct.

We analyzed the microarray datasets GSE78520 and GSE94508 to search for differentially expressed circRNAs associated with HCC. Expression of circSEC24A, microRNA (miR)-455-3p, and protein phosphatase, Mg2+/Mn2+ dependent 1F (PPM1F) mRNA was detected by quantitative real-time polymerase chain reaction (RT-qPCR). Loss-of-function experiments were conducted to validate the biological function of circSEC24A in HCC cells in vitro and in vivo. Protein levels were evaluated by western blotting and immunohistochemistry (IHC). The relationship between circSEC24A or PPM1F and miR-455-3p was verified by a dual-luciferase reporter and/or RNA immunoprecipitation (RIP) assays.

circSEC24A was overexpressed in HCC. circSEC24A silencing decreased xenograft tumor growth in vivo and repressed proliferation, metastasis, invasion, epithelial-to-mesenchymal transition (EMT), induced cell cycle arrest, and apoptosis of HCC cells in vitro. circSEC24A acted as a molecular sponge to sequester miR-455-3p, resulting in elevating the expression of PPM1F. miR-455-3p inhibitor reversed the suppressive impact of circSEC24A silencing on malignant behaviors of HCC cells. PPM1F overexpression offsets the inhibitory effect of miR-455-3p mimic on malignant behaviors of HCC cells.

circSEC24A sponged miR-455-3p to elevate the PPM1F expression, resulting in accelerating malignant behaviors of HCC cells. The study provided a potential therapeutic target for patients with HCC.

Key words: HCC; circSEC24A; miR-455-3p; PPM1F

Hepatocellular carcinoma (HCC) ranks third in the cause of death due to cancer [1]. The occurrence of HCC is closely related to chronic hepatitis, especially chronic viral hepatitis infection (hepatitis B or C) [2]. Most HCC patients are diagnosed at an advanced stage and are not suitable for surgical treatment [3]. Also, patients with advanced HCC have an extremely poor prognosis [4]. Thus, studying the underlying molecular mechanisms of HCC development is essential to provide guidance for the exploitation of HCC treatment tactics.

Circular RNAs (circRNAs) are endogenous RNA molecules with unique circular structures. They are derived from pre-mRNA through back-splicing and have the ability to resist RNase R digestion [5]. CircRNAs are emerging as vital regulators of gene expression and cellular functions [6]. Mounting reports have uncovered that circRNAs are implicated in the development of HCC [7]. For example, circRNA circLRIG3 drove tumor progression through regulation of the EZH2/STAT3 signaling [8]. Moreover, circRNA circSORE sustained cell chemoresistance through activating the Wnt/β-catenin pathway in HCC [9]. Also, circRNA circBACH1 repressed p27 expression by interacting with HuR, resulting in accelerating cell growth in HCC [10]. Hsa_circ_0003528 (circSEC24A), located at chr5: 134032815-134044578, is generated by the SEC24 Homolog A, COPII Coat Complex Component (SEC24A) gene. Huang et al. discovered that circSEC24A contributed to the polarization of tuberculosis-related macrophages [11]. In addition, circSEC24A had been revealed to be upregulated in liver cancer (GSE78520 and GSE94508). However, the function of circSEC24A in cancer and HCC has not been validated.

Studies have demonstrated that circRNAs can sequester microRNAs (miRs) by miR response elements, thus regulating downstream targets of miRs [12, 13]. MiR-455-3p is encoded by the COL27A1 gene [14]. Abnormal miR-455-3p expression is related to a variety of human diseases, such as osteoarthritis [15], pulmonary arterial hypertension [16], and cancer [17]. MiR-455-3p had been disclosed as a tumor repressor in HCC [18, 19]. Nevertheless, the mechanism of miR-455-3p dysregulation in HCC remains unclear. Members of the metal-dependent protein phosphatase (PPM) family are negative regulators of cellular stress response pathways, such as HOG, JNK, and p38 MAPK signaling pathways [20]. Mg^{2+}/Mn^{2+}-dependent protein phosphatase 1F (PPM1F), a serine/threonine protein phosphatase, belongs to the PPM family. PPM1F is implicated in cancer cell motility and adhesion [21, 22]. Also, PPM1F plays dual regulatory functions in cancer cell

metastasis [23]. In gastric cancer, PPM1F had been unmasked as a suppressive factor [24], while PPM1F was proved as an oncogene in HCC [25, 26]. At present, the connection between miR-455-3p and PPM1F in HCC is unclear.

In the research, circSEC24A was confirmed to exert an oncogenic role in HCC. Moreover, circSEC24A elevated PPM1F expression by sequestering miR-455-3p, thus accelerating HCC cell proliferation, metastasis, invasion, and EMT.

Patients and methods

Clinical specimens and ethics approval. Paired HCC tissues and periphery (peri)-tumor tissues were collected from the Sichuan Cancer Hospital and Institute. All registered HCC patients had signed informed consents and had never suffered other tumors. The current research was ratified by the Ethics Committee of the Sichuan Cancer Hospital and Institute.

Cell culture. 293T cells and normal liver cells (THLE-2) were purchased from Mingzhou Biotechnology (Ningbo, China). HCC cells (Huh7, SK-Hep-1, Hep3B, and Bel-7405) were bought from Procell (Wuhan, China). These cells were cultured in Dulbecco's Modified Eagle Medium (Procell) (Huh7 and 293T cells), Minimum Essential Medium (Thermo Fisher, Carlsbad, CA, USA) (SK-Hep-1 and Hep3B cells), or Roswell Park Memorial Institute-1640 Medium (Thermo Fisher) (Bel-7405 and THLE-2 cells) supplemented with fetal bovine serum (FBS) (Thermo Fisher) and 1% Penicillin/Streptomycin (Thermo Fisher) under suitable conditions (95% relative humidity, 5% carbon dioxide, and 37 °C).

Oligonucleotides, plasmids, and transfection. Small interference (si) RNAs (si-circSEC24A#1, si-circSEC24A#2, and si-circSEC24A#3) that were used to silence endogenous circSEC24A expression, negative control for siRNAs (si-NC), short hairpin (sh) RNA against circSEC24A (sh-circSEC24A), negative control for shRNA (sh-NC), miR-455-3p inhibitor, negative control for miR-455-3p inhibitor (inhibitor NC), miR-455-3p mimic, and negative control for miR-455-3p mimic (mimic NC) were synthesized by RiboBio (Guangzhou, China). Overexpression plasmid of PPM1F (pcDNA-PPM1F) was constructed with the pcDNA vector (Thermo Fisher). Liposomal cocktails with oligonucleotides or/and plasmids were generated with Lipofectamine 3000 (Thermo Fisher). Transfected cells were harvested and used in subsequent experiments.

Quantitative real-time polymerase chain reaction (RT-qPCR). The TRIzol™ Plus RNA

Purification Kit (Thermo Fisher) was utilized for total RNA isolation. RNase R treatment was carried out at 37 °C with 3 U/μg RNase R (BioVision, Milpitas, CA, USA). Reverse transcription was performed using Prime Script™ RT reagent kit (TaKaRa, Dalian, China) or miRscript cDNA synthesis kit (QIAGEN, Hilden, Germany). qPCR was set up with the SYBR Premix Ex Taq Kit (Applied Biosystems, Foster City, CA, USA) in triplicate and the primers utilized in the present research were exhibited in Table 1. U6 or GAPDH was used as an endogenous reference. Data was figured with the $2^{-\Delta\Delta Ct}$ method.

Cell counting kit-8 (CCK-8) assay. Treated HCC cells (about 2×10^3) were cultured in 96-well plates. After incubation with CCK-8 solution (10 μl, Dojindo, Kumamoto, Japan), the optical density (OD) value was read with the spectrophotometer reader (Thermo Fisher) at a wavelength of 450 nm.

Colony formation assay. Treated HCC cells (approximately 2×10^3) were seeded into 6-well plates. The colonies were stained with crystal violet solution (Sigma, St. Louis, MO, USA) (0.5% crystal violet in 10% methanol and 90% water) and then counted with a microscope (Olympus, Tokyo, Japan).

Flow cytometry assay. HCC cells in the logarithmic phase were harvested and fixed with cold 70% ethanol. Subsequently, the cells were digested with 2 μg RNase A (Sigma,) and then labeled with 15 μg/ml propidium iodide (PI) (Beyotime, Jiangsu, China) for 15 min. The cell cycle distribution was analyzed using the FACS Calibur flow cytometer (Becton Dickinson, San Jose, California, USA). Cell apoptosis analysis was carried out according to the instructions of the Annexin V-FITC/PI apoptosis detection kit (Sigma).

5-ethynyl-2'-deoxyuridine (EDU) assay. EDU assay was conducted with the Cell-Light EdU Apollo 567 In Vitro Imaging Kit (RiboBio, Guangzhou, China) based on the manufacturer's instructions. Images were captured by the microscope (Olympus). EDU-positive cells were labeled with red fluorescence, while nuclei were labeled with DAPI (4,6-diamidino-2-phenylindole; blue).

Transwell assay. The metastasis and invasion of HCC cells were analyzed by transwell assay with transwell chambers with (#354480, Costar, Cambridge, MA, USA) or without Matrigel. In short, treated HCC cells (5×10^4) in a serum-free medium were seeded onto the apical chamber. 24 h after seeding, the migrated and invaded cells were stained with 0.5% crystal violet (Sigma) and then counted in 5 randomly selected fields using a microscope (Olympus).

Western blotting. Total protein was extracted using the RIPA buffer (Beyotime) and then isolated with 10% sodium dodecyl sulfate-polyacrylamide gel electrophoresis. After transferring to the polyvinylidene fluoride (PVDF) membrane (Millipore, Bedford, MA, USA) and sealing with 5% skimmed milk powder, the membranes were incubated with the appropriate primary antibodies against E-cadherin (1:600, ab1416), Vimentin (1:1000, ab8978), PPM1F (1:1000, ab200394), and GAPDH (1:2500, ab8245), followed by washing and incubating with the appropriate peroxidase secondary antibody. These antibodies were purchased from Abcam (Cambridge, MA, USA). Bands were detected using the Pierce™ ECL WB Substrate (Thermo Fisher) and visualized after exposure onto HyBlot CL Autoradiography Film (Denville Scientific, Metuchen, NJ USA).

Dual-luciferase reporter assay. The binding sites of circSEC24A and PPM1F 3' untranslated region (UTR) in miR-455-3p were predicted using the starBase database. The wild type sequences of circSEC24A and PPM1F 3'UTR and their mutant sequences were inserted into the pMIR-REPORT vector (Applied Biosystems) to construct a luciferase vector carrying circSEC24A wt, PPM1F 3'UTR wt, circSEC24A mut, or PPM1F 3'UTR mut, respectively. Following this, 293T cells were transfected with mimic NC or miR-455-3p mimic together with a luciferase vector, followed by analyzing luciferase activities using the Pierce™ Renilla-Firefly Luciferase Dual Assay Kit (Thermo Fisher) based on the manufacturer's instructions on an LD400 luminescence detector (Beckman Coulter, Brea, CA, USA).

RNA immunoprecipitation (RIP) analysis. The interaction between circSEC24A and miR-455-3p was verified with the Magna RIP kit (Millipore) in accordance with the instructions from the manufacturer. Abundance of circSEC24A and miR-455-3p in precipitated RNAs was assessed through carrying out RT-qPCR analysis.

Xenograft assay. 14 BALB/c nude mice (Vital River Laboratory, Beijing, China) were manipulated based on protocols approved by the Animal Care Committee of Sichuan Cancer Hospital and Institute. Briefly, Hep3B cells carrying lentivirus-mediated sh-circSEC24A or sh-NC were subcutaneously injected into nude mice. The size of tumor was measured once a week (Volume=(length $\times$width^2)/2). All mice were sacrificed after 35 days, and xenograft tumors were stripped and weighed, followed by embedding in paraffin for immunohistochemistry (IHC) staining.

Statistical analysis. Statistical analyses were conducted using SPSS Statistics software version 17.0

(SPSS, Chicago, IL, USA). For *in vivo* and *in vitro* experiments, the Student's *t*-test or one-way analysis of variance was utilized to evaluate the difference between two or among multiple groups. $P < 0.05$ was considered statistically significant. All data were presented as mean±standard deviation from at least three repeats. Each experiment was conducted in triplicate.

Results

CircSEC24A was highly expressed in HCC. To search for differentially expressed circRNAs related to HCC, we analyzed microarray datasets (GSE78520 and GSE94508) concerning the circRNA profiles in liver cancer tissues. We found that there were 5 overlapping circRNAs (hsa_circ_0067934, hsa_circ_0003528, hsa_circ_0001955, hsa_circ_0008274, and hsa_circ_0072088) in the top 50 upregulated circRNAs in the GSE78520 and GSE94508 microarray datasets (Figure 1A). Among the 5 overlapping circRNAs, the biological role of hsa_circ_0067934 [27], hsa_circ_0001955 [28], hsa_circ_0008274 [29], and hsa_circ_0072088 [30] in HCC had been verified. Thus, we choose hsa_circ_0003528 for further exploration. Hsa_circ_0003528 (circSEC24A) is formed by reverse splicing of exon 14 to exon 18 (741 bp) of the SEC24A gene (Figure 1B). To verify the expression tendency of circSEC24A in 40 paired HCC tissues and peri-tumor tissues, RT-qPCR was performed. As presented in Figure 1C, circSEC24A expression was observably elevated in HCC tissues in contrast to peri-tumor tissues. Furthermore, the Kaplan-Meier curve showed that HCC patients with high circSEC24A expression had a shorter survival time than those with low circSEC24A expression (Figure 1D). As expected, circSEC24A was upregulated in HCC cells (Huh7, SK-Hep-1, Hep3B, and Bel-7405) than that in the THEL-2 cells (Figure 1E). Then, RNase R treatment was performed to validate the circular structure of circSEC24A. RT-qPCR exhibited that linear SEC24A was digested after RNase R treatment, but circular SEC24A did not change. The digestion resistance of circSEC24A to RNase R confirmed its closed-loop structure (Figure 1F). These results indicated that high circSEC24A expression might be associated with the progression of HCC.

CircSEC24A accelerated HCC cell proliferation, metastasis, invasion, and EMT. Based on the upregulation of circSEC24A in HCC, we investigated the biological function of circSEC24A by loss-of-function experiments. Three siRNAs (si-circSEC24A#1, si-circSEC24A#2, and si-circSEC24A#3) against the reverse splice region of circSEC24A were designed and transfected

into HCC cells. The knockdown efficiencies of three siRNAs were exhibited in Fig. 2A. CCK-8 and colony formation assays indicated that circSEC24A silencing constrained growth and colony formation of Huh7 and Hep3B cells (Figures 2B-2D). Cell cycle analysis revealed that circSEC24A inhibition elevated the proportion of Huh7 and Hep3B cells in the G0/G1 stage and decreased the proportion of Huh7 and Hep3B cells in the S stage, illustrating circSEC24A knockdown induced cell cycle arrest in Huh7 and Hep3B cells (Figures 2E, 2F). EDU assay exhibited that circSEC24A inhibition decreased the proportion of EDU-positive Huh7 and Hep3B cells (Figures 2G, 2H). Cell apoptosis analysis presented that the proportion of apoptotic Huh7 and Hep3B cells was increased after circSEC24A silencing (Figures 2I, 2J). Transwell assay showed that the inhibition of circSEC24A decreased the number of migrated and invaded Huh7 and Hep3B cells (Figures 2K-2N). Moreover, circSEC24A silencing elevated E-cadherin protein level and decreased Vimentin protein level in Huh7 and Hep3B cells (Figures 2O, 2P). These results manifested that circSEC24A facilitated HCC cell proliferation, metastasis, invasion, and EMT *in vitro*.

CircSEC24A was validated as a miR-455-3p sponge. Many studies have revealed that circRNAs can function as miR sponges in tumor development. By analyzing the starBase database, we discovered that miR-455-3p might interact with circSEC24A and the binding sites of circSEC24A in miR-455-3p were presented in Figure 3A. Dual-luciferase reporter assay exhibited that the luciferase activity of the circSEC24A wt reporter was repressed in miR-455-3p mimic-transfected 293T cells (Figure 3B). RIP assay presented that circSEC24A and miR-455-3p could be co-enriched in the anti-Ago2 group compared to the IgG group (Figure 3C). As expected, there was a significant downregulation of miR-455-3p in HCC tissues and cells (Figures 3D, 3E). Also, the expression of circSEC24A was negatively correlated with miR-455-3p in HCC tissues (Figure 3F). Together, these results manifested that circSEC24A served as a sponge for miR-455-3p.

CircSEC24A promoted HCC cell proliferation, metastasis, invasion, and EMT via sponging miR-455-3p. As we previously proved that circSEC24A acted as a miR-455-3p decoy, we hypothesized that circSEC24A inhibition might reduce HCC cell proliferation, metastasis, invasion, and EMT via sponging miR-455-3p. The silence efficiency of miR-455-3p inhibitor in Huh7 and Hep3B cells was verified by RT-qPCR (Figure 4A). Moreover, miR-455-3p inhibitor reversed the upregulation of miR-455-3p in circSEC24A-silenced Huh7 and Hep3B cells (Figure 4B). Also, miR-455-3p inhibitor offset circSEC24A knockdown-mediated repressive influence on growth,

colony formation, cell cycle progression, and proliferation of Huh7 and Hep3B cells (Figures 4C-4F). Furthermore, the elevation of the proportion of apoptotic Huh7 and Hep3B cells caused by circSEC24A silencing was overturned after miR-455-3p inhibition (Figure 4G). Additionally, miR-455-3p inhibitor counteracted the suppressive effect of circSEC24A knockdown on migration and invasion of Huh7 and Hep3B cells (Figures 4H-4K). As expected, miR-455-3p inhibitor reversed the upregulation of E-cadherin protein and downregulation of Vimentin protein in circSEC24A-silenced Huh7 and Hep3B cells (Figures 4L, 4M). Collectively, these results illustrated that circSEC24A accelerated proliferation, metastasis, invasion, and EMT of HCC cells via sponging miR-455-3p.

PPM1F acted as a miR-455-3p target. Based on the competing endogenous RNA (ceRNA) hypothesis, circRNA can relieve the suppressive influence of miR on its target by functioning as a miR sponge. Thus, we identified the potential target of miR-455-3p with the starbase database. As exhibited in Figure 5A, PPM1F might be a target of miR-455-3p. The luciferase activity of the PPM1F 3'UTR wt reporter was impaired by miR-455-3p mimic compared with the control group, but the luciferase activity of the PPM1F 3'UTR mut reporter did not change (Figure 5B). Results of RT-qPCR and western blotting revealed that the levels of PPM1F mRNA and protein were upregulated in HCC tissues compared to peri-tumor tissues (Figures 5C, 5D). Also, the level of PPM1F protein was upregulated in HCC cells (Figure 5E). Furthermore, there was a negative correlation between PPM1F mRNA and miR-455-3p expression in HCC tissues (Figure 5F). The decrease in PPM1F expression in si-circSEC24A#1-transfected Huh7 and Hep3B cells was reversed by miR-455-3p inhibitor (Figure 5G). Thus, these results indicated that circSEC24A regulated PPM1F expression through serving as a miR-455-3p sponge.

MiR-455-3p repressed proliferation, metastasis, invasion, and EMT of HCC cells by targeting PPMF1. To investigate whether miR-455-3p played its function through targeting PPMF1 in HCC cells, rescue experiments were conducted by transfecting pcDNA-PPMF1 into Huh7 and Hep3B cells carrying miR-455-3p mimic. The overexpression efficiencies of miR-455-3p mimic and pcDNA-PPMF1 in Huh7 and Hep3B cells were verified by RT-qPCR and western blotting, respectively (Figures 6A, 6B). The transfection of pcDNA-PPMF1 restored the downregulation of PPMF1 protein in Huh7 and Hep3B cells carrying miR-455-3p mimic (Figure 6C). Moreover, PPMF1 overexpression overturned the inhibitory effect of miR-455-3p mimic on growth, colony

formation, cell cycle progression, and proliferation of Huh7 and Hep3B cells (Figures 6D-6G). Furthermore, miR-455-3p mimic induced cell apoptosis and repressed cell metastasis and invasion in Huh7 and Hep3B cells, but these impacts mediated by miR-455-3p mimic was offset after pcDNA-PPMF1 introduction (Figures 6H-6L). In addition, miR-455-3p mimic elevated the E-cadherin protein level and decreased the Vimentin protein level in Huh7 and Hep3B cells, but these trends caused by miR-455-3p mimic were reversed by forcing PPMF1 expression (Figures 6M, 6N). In summary, miR-455-3p repressed HCC cell proliferation, metastasis, invasion, and EMT via targeting PPMF1.

CircSEC24A knockdown repressed HCC growth *in vivo*. To further validate the function of circSEC24A in HCC progression, Hep3B cells carrying lentivirus-mediated sh-circSEC24A or sh-NC were subcutaneously injected into BALB/c nude mice. The results showed that tumor volume and weight in the sh-circSEC24A growth were smaller and lower compared with the sh-NC group (Figures 7A, 7B). As expected, the expression of circSEC24A and PPMF1 mRNA was downregulated in mice tumor tissues in the sh-circSEC24A group in contrast to the sh-NC group, but miR-455-3p expression was upregulated (Figure 7C). IHC analysis displayed that PPM1F and Vimentin protein levels were downregulated in mice tumor tissues in the sh-circSEC24A group, but the E-cadherin protein level was upregulated (Figure 7D). Together, the downregulation of circSEC24A curbed HCC growth *in vivo*.

Discussion

A series of studies have found that differential circRNA expression is related to the clinical characteristics of cancer patients [31, 32]. Also, circRNAs provide a new direction for studying tumor pathogenesis and potential therapeutic targets [33]. Herein, we demonstrated that circSEC24A played an oncogenic role through sequestering miR-455-3p and upregulating PPM1F in HCC, offering evidence to support circSEC24A as an underlying therapeutic target for HCC.

The host gene of circSEC24A is SEC24A. SEC24A, a cytosolic protein, plays a fundamental role in coat protein complex II (COPII)-dependent endoplasmic reticulum-Golgi protein transport [34]. Furthermore, the intracellular transport of hepatitis B subviral envelope particles depends on the COPII mechanism through the selective utilization of SEC24A and SEC23B [35]. Also, SEC24A had been uncovered to play a promoting impact on gastric cancer cell invasion and metastasis [36].

A recent report revealed that circSEC24A facilitated mycobacterium tuberculosis-related macrophage polarization via upregulating CTLA4. These data offered evidence for the function of circSEC24A. In this study, circSEC24A was highly expressed in HCC. And HCC patients with high circSEC24A expression had a shorter survival time than those with low circSEC24A expression, manifesting that circSEC24A might be a potential biomarker for analyzing the prognosis of HCC patients. Moreover, circSEC24A silencing constrained xenograft tumor growth and repressed HCC cell proliferation, metastasis, invasion, and EMT *in vitro*. Thus, these data indicated that circSEC24A exerted a promoting effect on tumor progression in HCC.

Given that circRNAs can interact with miRs via miR response elements. Through a series of validation, circSEC24A was validated as a miR-455-3p decoy. Report of Lan et al. discovered that miR-455-3p downregulation-mediated STK17B upregulation activated the AKT/GSK-3β/Snail signaling, thus promoting tumorigenesis and metastasis in HCC [18]. It was reported that miR-455-3p played an antagonistic effect on liver Fibrosis by targeting HSF1 [37]. Moreover, TUG1 sequestered miR-455-3p and elevated AMPKβ2 expression, resulting in promoting cell metastasis and glycolysis through in HCC [19]. Herein, miR-455-3p downregulation overturned circSEC24A downregulation-mediated impacts on malignant behaviors of HCC cells. Consequently, we deduced that circSEC24A contributed to HCC cell malignancy via serving as a miR-455-3p sponge.

PPM1F, a serine/threonine phosphatase, takes part in the progression of human cancers [38]. A previous study revealed that miR-590-3p promoted invasion and proliferation through targeting PPM1F in gastric cancer [24]. In addition, Jurmeister et al. exposed that miR-200c inhibited cell metastasis through downregulating FHOD1 and PPM1F [39]. In HCC, circRNA circSLC3A2 promoted cell invasion and proliferation through adsorbing miR-490-3p and upregulating PPM1F [26]. Also, SNHG8 contributed to metastasis, invasion, and proliferation through regulation of the miR-149-5p/PPM1F pathway [25]. Consistent with previous studies [25, 26], PPM1F was highly expressed in HCC. Forced miR-455-3p expression repressed cell malignant behaviors via decreasing PPM1F expression in HCC. Importantly, circSEC24A regulated PPM1F expression via adsorbing miR-455-3p. Thus, we concluded that circSEC24A promoted tumor growth by regulation of the miR-455-3p/PPM1F pathway in HCC.

In sum, circSEC24A was upregulated in HCC. Upregulation of circSEC24A adsorbed miR-455-3p

and increased PPM1F expression, thereby promoting tumor growth in HCC. The study manifested that circSEC24A was a promising target for HCC treatment.

References

[1] MILLER KD, NOGUEIRA L, MARIOTTO AB, ROWLAND JH, YABROFF KR et al. Cancer treatment and survivorship statistics, 2019. CA Cancer J Clin 2019; 69: 363-385. https://doi.org/10.3322/caac.21565

[2] ALTER MJ. Epidemiology of hepatitis C virus infection. World J Gastroenterol 2007; 13: 2436-2441.

[3] ESCUDIER B, WORDEN F, KUDO M. Sorafenib: key lessons from over 10 years of experience. Expert review of anticancer therapy 2019; 19: 177-189. https://doi.org/10.1080/14737140.2019.1559058

[4] DISTEFANO JK, DAVIS B. Diagnostic and Prognostic Potential of AKR1B10 in Human Hepatocellular Carcinoma. Cancers (Basel) 2019; 11. https://doi.org/10.3390/cancers11040486

[5] GAN H, LEI Y, YUAN N, TANG K, HAO W et al. Circular RNAs in depression: Biogenesis, function, expression, and therapeutic potential. Biomed Pharmacother 2021; 137: 111244. https://doi.org/10.1016/j.biopha.2021.111244

[6] RAJAPPA A, BANERJEE S, SHARMA V, KHANDELIA P. Circular RNAs: Emerging Role in Cancer Diagnostics and Therapeutics. Front Mol Biosci 2020; 7: 577938. https://doi.org/10.3389/fmolb.2020.577938

[7] CHENG D, WANG J, DONG Z, LI X. Cancer-related circular RNA: diverse biological functions. Cancer Cell Int 2021; 21: 11. https://doi.org/10.1186/s12935-020-01703-z

[8] SUN S, GAO J, ZHOU S, LI Y, WANG Y et al. A novel circular RNA circ-LRIG3 facilitates the malignant progression of hepatocellular carcinoma by modulating the EZH2/STAT3 signaling. J Exp Clin Cancer Res 2020; 39: 252. https://doi.org/10.1186/s13046-020-01779-5

[9] XU J, WAN Z, TANG M, LIN Z, JIANG S et al. N-methyladenosine-modified CircRNA-SORE sustains sorafenib resistance in hepatocellular carcinoma by regulating β-catenin signaling. Mol Cancer 2020; 19: 163. https://doi.org/10.1186/s12943-020-01281-8

[10] LIU B, YANG G, WANG X, LIU J, LU Z et al. CircBACH1 (hsa_circ_0061395) promotes hepatocellular carcinoma growth by regulating p27 repression via HuR. J Cell Physiol 2020; 235: 6929-6941. https://doi.org/10.1002/jcp.29589

[11] HUANG Z, YAO F, LIU J, XU J, GUO Y et al. Up-regulation of circRNA-0003528 promotes mycobacterium tuberculosis associated macrophage polarization via down-regulating miR-224-5p, miR-324-5p and miR-488-5p and up-regulating CTLA4. Aging (Albany NY) 2020; 12: 25658-25672. https://doi.org/10.18632/aging.104175

[12] HAN TS, HUR K, CHO HS, BAN HS. Epigenetic Associations between lncRNA/circRNA and miRNA in Hepatocellular Carcinoma. Cancers (Basel) 2020; 12. https://doi.org/10.3390/cancers12092622

[13] TAY Y, RINN J, PANDOLFI PP. The multilayered complexity of ceRNA crosstalk and competition. Nature 2014; 505: 344-352. https://doi.org/10.1038/nature12986

[14] KUMAR S, REDDY PH. A New Discovery of MicroRNA-455-3p in Alzheimer's Disease. J Alzheimers Dis 2019; 72: S117-S130. https://doi.org/10.3233/JAD-190583

[15] HU S, ZHAO X, MAO G, ZHANG Z, WEN X et al. MicroRNA-455-3p promotes TGF-β signaling and inhibits osteoarthritis development by directly targeting PAK2. Exp Mol Med 2019; 51: 1-13. https://doi.org/10.1038/s12276-019-0322-3

[16] ZHOU C, CHEN Y, KANG W, LV H, FANG Z et al. Mir-455-3p-1 represses FGF7 expression to inhibit pulmonary arterial hypertension through inhibiting the RAS/ERK signaling pathway. J Mol Cell Cardiol 2019; 130: 23-35. https://doi.org/10.1016/j.yjmcc.2019.03.002

[17] LIU A, ZHU J, WU G, CAO L, TAN Z et al. Antagonizing miR-455-3p inhibits chemoresistance and aggressiveness in esophageal squamous cell carcinoma. Mol Cancer 2017; 16: 106. https://doi.org/10.1186/s12943-017-0669-9

[18] LAN Y, HAN J, WANG Y, WANG J, YANG G et al. STK17B promotes carcinogenesis and metastasis via AKT/GSK-3β/Snail signaling in hepatocellular carcinoma. Cell Death Dis 2018; 9: 236. https://doi.org/10.1038/s41419-018-0262-1

[19] LIN YH, WU MH, HUANG YH, YEH CT, CHENG ML et al. Taurine up-regulated gene 1 functions as a master regulator to coordinate glycolysis and metastasis in hepatocellular carcinoma. Hepatology 2018; 67: 188-203. https://doi.org/10.1002/hep.29462

[20] HANADA M, NINOMIYA-TSUJI J, KOMAKI K, OHNISHI M, KATSURA K et al. Regulation of the TAK1 signaling pathway by protein phosphatase 2C. J Biol Chem 2001; 276: 5753-5759. https://doi.org/10.1074/jbc.M007773200

[21] SUSILA A, CHAN H, LOH AXW, PHANG HQ, WONG ET et al. The POPX2 phosphatase regulates cancer cell motility and invasiveness. Cell Cycle 2010; 9: 179-187. https://doi.org/10.4161/cc.9.1.10406

[22] SINGH P, GAN CS, GUO T, PHANG H-Q, SZE SK et al. Investigation of POPX2 phosphatase functions by comparative phosphoproteomic analysis. Proteomics 2011; 11: 2891-2900. https://doi.org/10.1002/pmic.201100044

[23] ZHANG S, WENG T, CHERUBA E, GUO T, CHAN H et al. Phosphatase POPX2 Exhibits Dual Regulatory Functions in Cancer Metastasis. J Proteome Res 2017; 16: 698-711. https://doi.org/10.1021/acs.jproteome.6b00748

[24] ZHANG J, JIN M, CHEN X, ZHANG R, HUANG Y et al. Loss of PPM1F expression predicts tumour recurrence and is negatively regulated by miR-590-3p in gastric cancer. Cell Prolif 2018; 51: e12444. https://doi.org/10.1111/cpr.12444

[25] DONG J, TENG F, GUO W, YANG J, DING G et al. lncRNA SNHG8 Promotes the Tumorigenesis and Metastasis by Sponging miR-149-5p and Predicts Tumor Recurrence in Hepatocellular Carcinoma. Cell Physiol Biochem 2018; 51: 2262-2274. https://doi.org/10.1159/000495871

[26] WANG H, CHEN W, JIN M, HOU L, CHEN X et al. CircSLC3A2 functions as an oncogenic factor in hepatocellular carcinoma by sponging miR-490-3p and regulating PPM1F expression. Mol Cancer 2018; 17: 165. https://doi.org/10.1186/s12943-018-0909-7

[27] ZHU Q, LU G, LUO Z, GUI F, WU J et al. CircRNA circ_0067934 promotes tumor growth and metastasis in hepatocellular carcinoma through regulation of miR-1324/FZD5/Wnt/β-catenin axis. Biochem Biophys Res Commun 2018; 497: 626-632. https://doi.org/10.1016/j.bbrc.2018.02.119

[28] DING B, FAN W, LOU W. hsa_circ_0001955 Enhances Proliferation, Migration, and Invasion of HCC Cells through miR-145-5p/NRAS Axis. Mol Ther Nucleic Acids 2020; 22: 445-455. https://doi.org/10.1016/j.omtn.2020.09.007
[29] KONG Q, FAN Q, MA X, LI J, MA R. CircRNA circUGGT2 Contributes to Hepatocellular Carcinoma Development via Regulation of the miR-526b-5p/RAB1A Axis. Cancer Manag Res 2020; 12: 10229-10241. https://doi.org/10.2147/CMAR.S263985
[30] YANG X, LIU L, ZOU H, ZHENG Y-W, WANG K-P. circZFR promotes cell proliferation and migration by regulating miR-511/AKT1 axis in hepatocellular carcinoma. Dig Liver Dis 2019; 51: 1446-1455. https://doi.org/10.1016/j.dld.2019.04.012
[31] WANG M, YU F, LI P. Circular RNAs: Characteristics, Function and Clinical Significance in Hepatocellular Carcinoma. Cancers (Basel) 2018; 10: 258. https://doi.org/10.3390/cancers10080258
[32] JIANG YL, SHANG MM, DONG SZ, CHANG YC. Abnormally expressed circular RNAs as novel non-invasive biomarkers for hepatocellular carcinoma: A meta-analysis. World J Gastrointest Oncol 2019; 11: 909-924. https://doi.org/10.4251/wjgo.v11.i10.909
[33] BEILERLI A, GAREEV I, BEYLERLI O, YANG G, PAVLOV V et al. Circular RNAs as biomarkers and therapeutic targets in cancer. Semin Cancer Biol 2021; S1044-579X(21)00004-3. https://doi.org/10.1016/j.semcancer.2020.12.026
[34] SHARPE LJ, LUU W, BROWN AJ. Akt phosphorylates Sec24: new clues into the regulation of ER-to-Golgi trafficking. Traffic 2011; 12: 19-27. https://doi.org/10.1111/j.1600-0854.2010.01133.x
[35] ZEYEN L, DÖRING T, STIELER JT, PRANGE R. Hepatitis B subviral envelope particles use the COPII machinery for intracellular transport via selective exploitation of Sec24A and Sec23B. Cell Microbiol 2020; 22: e13181. https://doi.org/10.1111/cmi.13181
[36] LU M, WANG W, ZHANG S, LI Y. SEC24A stimulates oncogenicity of human gastric cancer cells. Int J Clin Exp Pathol 2018; 11: 4044-4051.
[37] WEI S, WANG Q, ZHOU H, QIU J, LI C et al. miR-455-3p Alleviates Hepatic Stellate Cell Activation and Liver Fibrosis by Suppressing HSF1 Expression. Mol Ther Nucleic Acids 2019; 16: 758-769. https://doi.org/10.1016/j.omtn.2019.05.001
[38] KIM PR, ZHANG S, RAHMAT MB, KOH C-G. Partners in crime: POPX2 phosphatase and its interacting proteins in cancer. Cell Death Dis 2020; 11: 840. https://doi.org/10.1038/s41419-020-03061-0
[39] JURMEISTER S, BAUMANN M, BALWIERZ A, KEKLIKOGLOU I, WARD A et al. MicroRNA-200c represses migration and invasion of breast cancer cells by targeting actin-regulatory proteins FHOD1 and PPM1F. Mol Cell Biol 2012; 32: 633-651. https://doi.org/10.1128/MCB.06212-11

Figure Legends

Figure 1. CircSEC24A was overexpressed in HCC. A) Venn diagram showed the overlapping circRNAs among the top 50 upregulated circRNAs in the GSE78520 and GSE94508 microarray datasets. B) Schematic illustration presented the formation of circSEC24A. C) RT-qPCR analysis of circSEC24A expression in 40 paired HCC tissues and peri-tumor tissues. D) Kaplan-Meier survival

curve and log-rank test were employed to assess the overall survival probability of HCC patients with high and low circSEC24A expression. Low and high circSEC24A expression was cut off by the median expression. E) Expression level of circSEC24A in HCC cells (Huh7, SK-Hep-1, Hep3B, and Bel-7405) and THEL-2 cells was detected by RT-qPCR. F) The circular structure of circSEC24A was verified by RNase R treatment and RT-qPCR analysis. *$p < 0.05$

Figure 2. CircSEC24A facilitated malignant behaviors of HCC cells. A) RT-qPCR verified the knockdown efficiency of si-circSEC24A#1, si-circSEC24A#2, and si-circSEC24A#3 in Huh7 and Hep3B cells. B-H) Influence of circSEC24A inhibition on growth, colony formation, cell cycle progression, and proliferation of Huh7 and Hep3B cells was analyzed by CCK-8, colony formation, flow cytometry, and EDU assays. I-N) Impacts of circSEC24A silencing on apoptosis, metastasis, and invasion of Huh7 and Hep3B cells were assessed by flow cytometry and transwell assays. O, P) Protein levels of E-cadherin and Vimentin in circSEC24A-repressed Huh7 and Hep3B cells were measured by western blotting. *$p < 0.05$

Figure 3. CircSEC24A served as a sponge for miR-455-3p. A) Schematic illustration presented the binding sites between circSEC24A and miR-455-3p. B) Dual-luciferase reporter detected the luciferase activity of the circSEC24A wt or circSEC24A mut reporter in 293T cells transfected with miR-455-3p mimic and miR-NC. C) RIP was verified to verify the interaction between circSEC24A and miR-455-3p. D, E) RT-qPCR detected the expression of miR-455-3p in HCC tissues and cells. F) Pearson's correlation analysis revealed the correlation between circSEC24A and miR-455-3p in HCC tissues. *$p < 0.05$

Figure 4. CircSEC24A adsorbed miR-455-3p to accelerate proliferation, metastasis, invasion, and EMT of HCC cells. A) RT-qPCR assessed the expression of miR-455-3p in Huh7 and Hep3B cells transfected with miR-455-3p inhibitor or inhibitor NC. B-M) Huh7 and Hep3B cells were transfected with si-NC, si-circSEC24A#1, si-circSEC24A#1+inhibitor NC, or si-circSEC24A#1+miR-455-3p inhibitor. (B) Analysis of the influence of miR-455-3p inhibitor on the expression of miR-455-3p in si-circSEC24A#1-transfected Huh7 and Hep3B cells by RT-qPCR. (C-F) Assessment of the effect of miR-455-3p inhibitor on growth, colony formation, cell cycle

progression, and proliferation of si-circSEC24A#1-transfected Huh7 and Hep3B cells by CCK-8, colony formation, flow cytometry, and EDU assays. G-K) Impacts of miR-455-3p inhibitor on apoptosis, metastasis, and invasion of si-circSEC24A#1-transfected Huh7 and Hep3B cells were analyzed by flow cytometry and transwell assays. L, M) Western blotting assessed the influence of miR-455-3p inhibitor on protein levels of E-cadherin and Vimentin in si-circSEC24A#1-transfected Huh7 and Hep3B cells. *$p < 0.05$

Figure 5. CircSEC24A sponged miR-455-3p to regulate PPM1F expression. A) The predicted binding sites between miR-455-3p and PPM1F 3'UTR. B) Dual-luciferase reporter assay was carried out to detect the luciferase activity in 293T cells co-transfected with miR-455-3p mimic or miR-NC and the PPM1F 3'UTR wt or PPM1F 3'UTR mut reporter C, D) The levels of PPM1F mRNA and protein in HCC tissues and peri-tumor tissues were analyzed by RT-qPCR or western blotting. E) Protein level of PPM1F in HCC cells was assessed by western blotting. F) The correlation between PPM1F mRNA and miR-455-3p expression in HCC was determined by Pearson's correlation analysis. G) Influence of miR-455-3p inhibitor on the level of PPM1F protein in si-circSEC24A#1-transfected Huh7 and Hep3B cells was analyzed by western blotting. *$p < 0.05$

Figure 6. MiR-455-3p constrained HCC cell proliferation, metastasis, invasion, and EMT via targeting PPMF1. A) RT-qPCR validated the overexpression efficiency of miR-455-3p mimic in Huh7 and Hep3B cells. B) Western blotting confirmed the overexpression efficiency of pcDNA-PPMF1 in Huh7 and Hep3B cells. C-N) Huh7 and Hep3B cells were transfected with mimic NC, miR-455-3p mimic, miR-455-3p mimic+pcDNA, or miR-455-3p mimic+pcDNA-PPMF1. C-G) Analysis of the influence of PPMF1 overexpression on growth, colony formation, cell cycle progression, and proliferation of Huh7 and Hep3B cells carrying miR-455-3p mimic by CCK-8, colony formation, flow cytometry, and EDU assays. H-L) Assessment of the effect of PPMF1 overexpression on apoptosis, metastasis, and invasion of Huh7 and Hep3B cells transfected with si-circSEC24A#1 by flow cytometry and transwell assays. M, N) Analysis of the effect of PPMF1 overexpression on protein levels of E-cadherin and Vimentin in si-circSEC24A#1-transfected Huh7 and Hep3B cells by western blotting. *$p < 0.05$

Figure 7. CircSEC24A silencing curbed HCC growth *in vivo*. A) Tumor volume was recorded once a week after mice injection with stable Hep3B cells. B) Average tumor weight was calculated after xenograft tumor removal. C) RT-qPCR was carried out to assess the expression levels of circSEC24A, miR-455-3p, and PPM1F mRNA in xenograft tumors. D) IHC analysis revealed protein levels of PPM1F, E-cadherin, and Vimentin in xenograft tumors. *$p < 0.05$

513 **Table 1.** Primer sequences used for RT-qPCR analysis.

Genes	Primer sequences (5'-3')
circSEC24A	Forward (F): 5'-GCCTGGACTCATGGTTCCTT-3'
	Reverse (R): 5'-TGCTGACCAGAACAGTCCAA-3'
SEC24A	F: 5'-AGCCCTGAAACCACGAGAGGAA-3'
	R: 5'-TGCTGACCAGAACAGTCCAAGG-3'
PPM1F	F: 5'-GCTGCTACAGACAGACCTTTCC-3'
	R: 5'-GGCGGTTAAAGAAACTCTGTGCC-3'
GAPDH	F: 5'-GTCTCCTCTGACTTCAACAGCG-3'
	R: 5'-ACCACCCTGTTGCTGTAGCCAA-3'
miR-455-3p	F: 5'-CGGCAGTCCATGGGCAT-3'
	R: 5'-AGTGCAGGGTCCGAGGTATT-3'
U6	F: 5'-CTCGCTTCGGCAGCACA-3'
	R: 5'-AACGCTTCACGAATTTGCGT-3'

514

Fig. 1 Download full resolution image

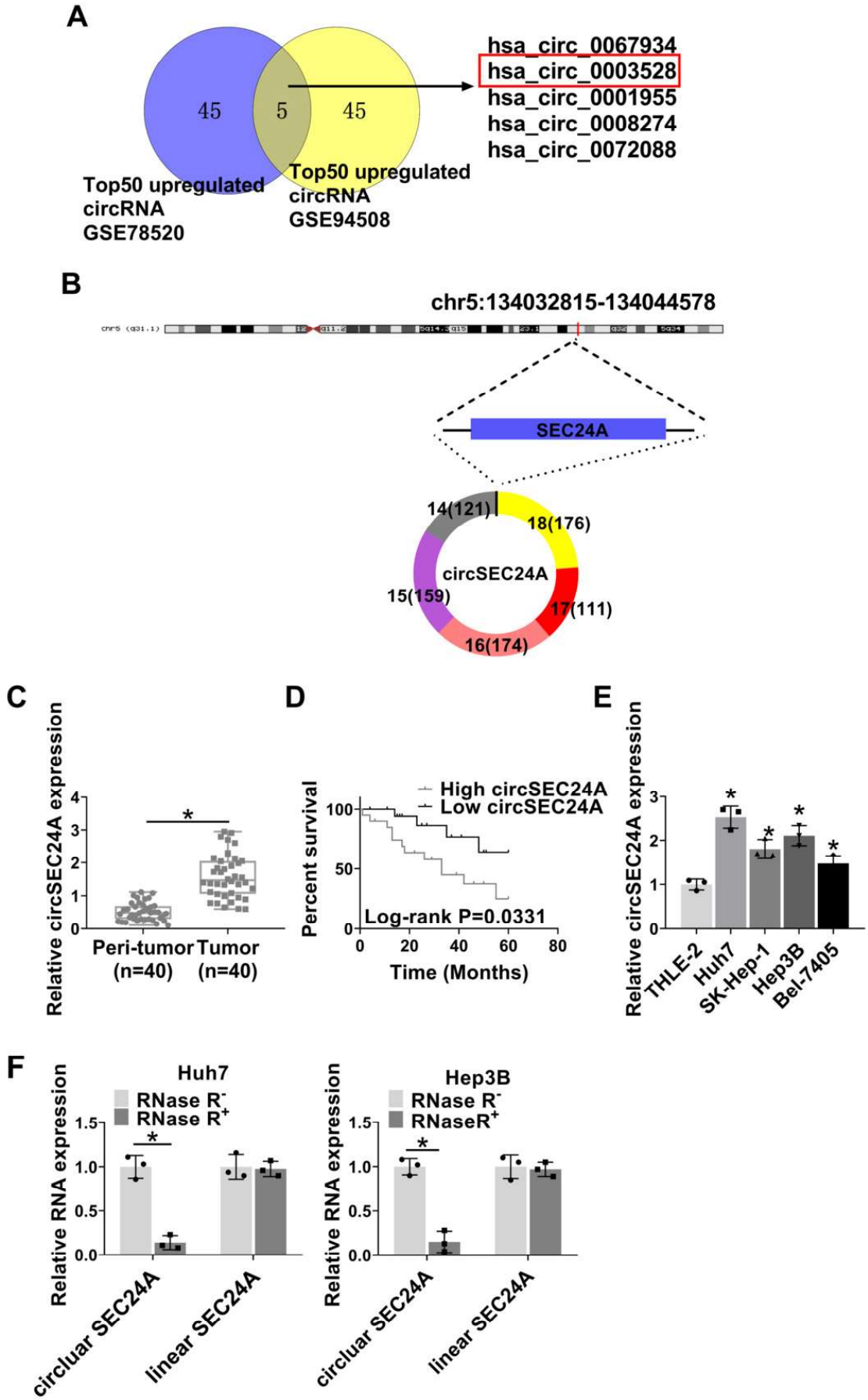

Fig. 2 [Download full resolution image]

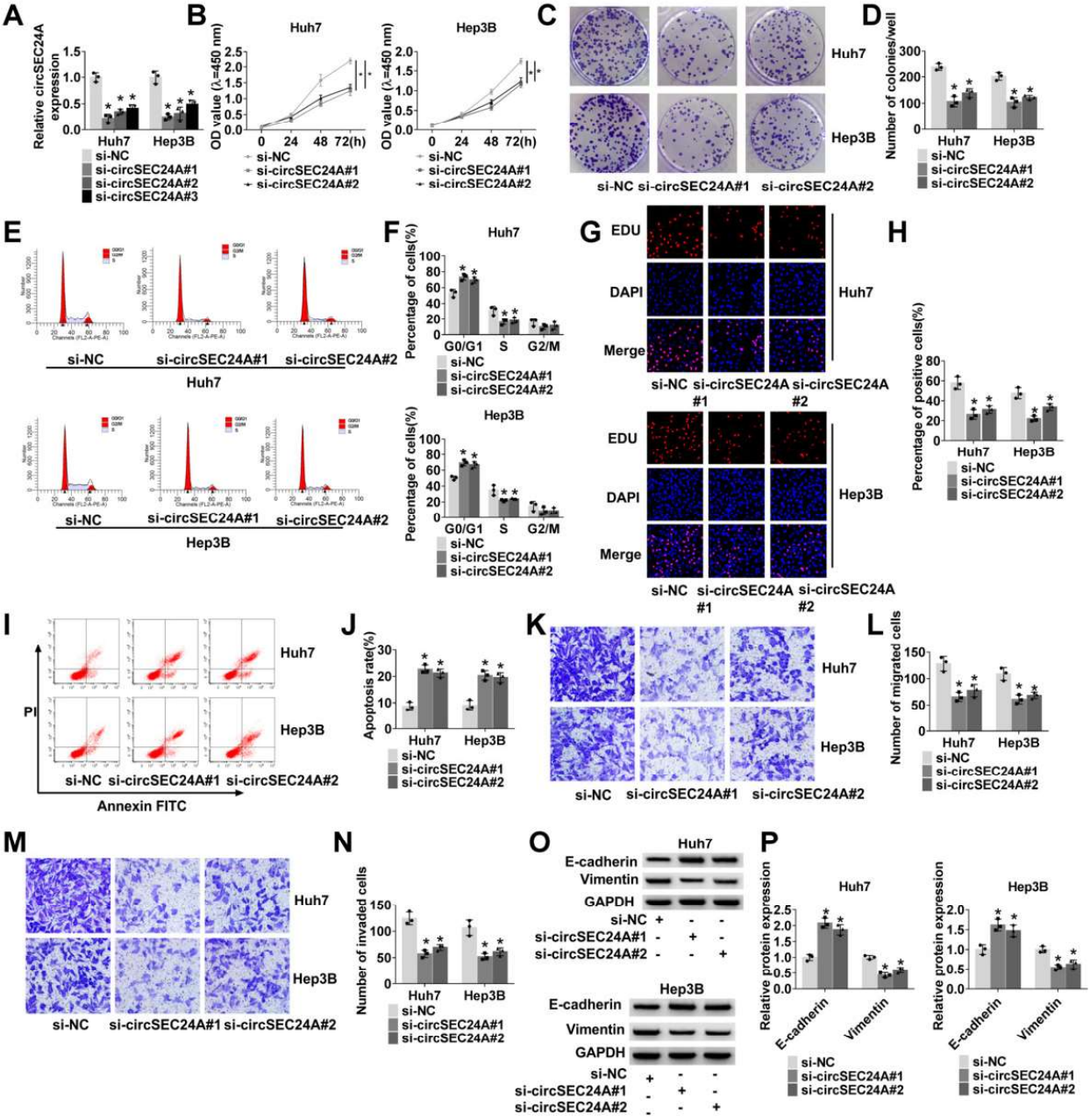

Fig. 3 Download full resolution image

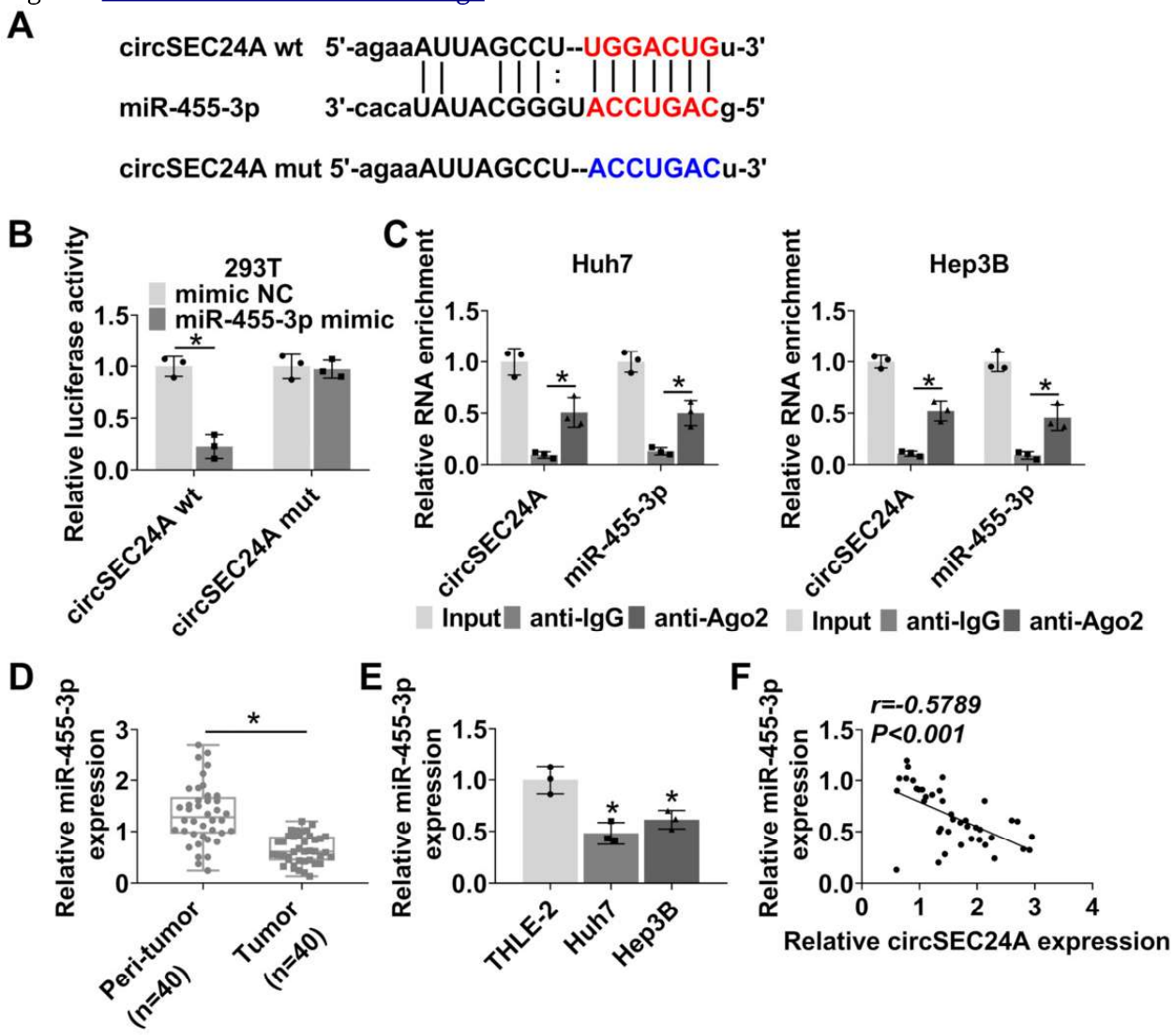

Fig. 4 [Download full resolution image]

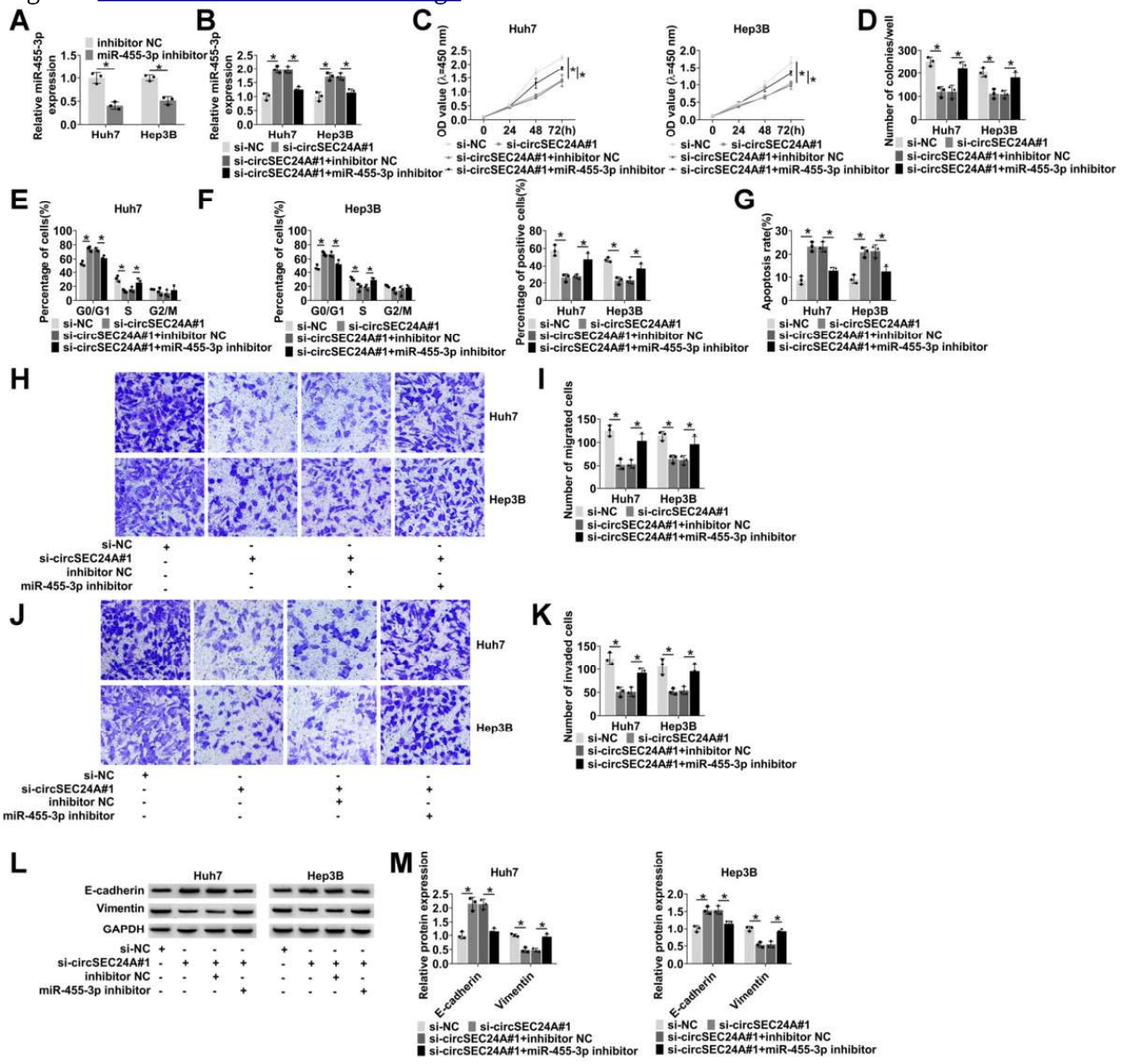

Fig. 5 Download full resolution image

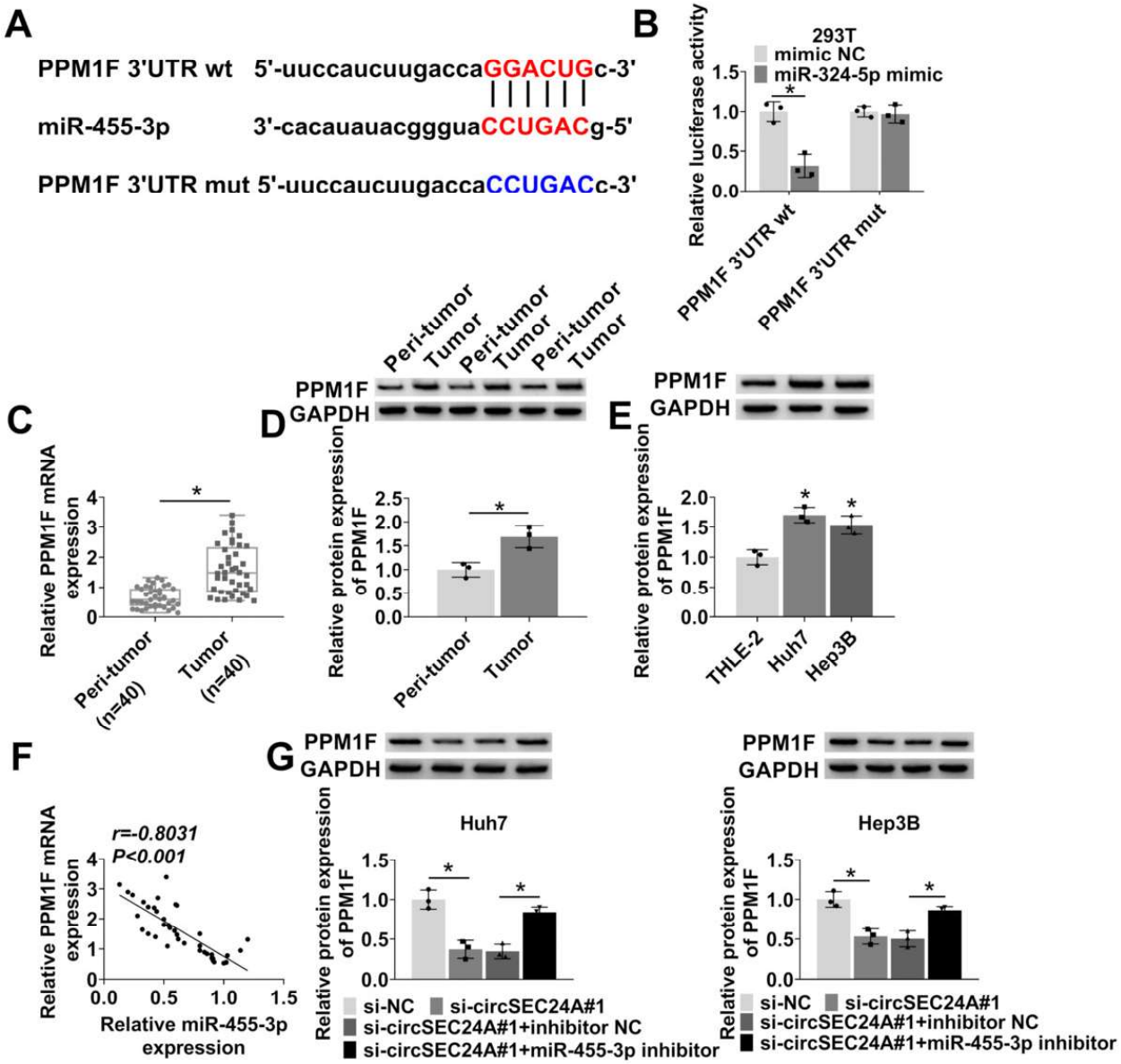

Fig. 6 Download full resolution image

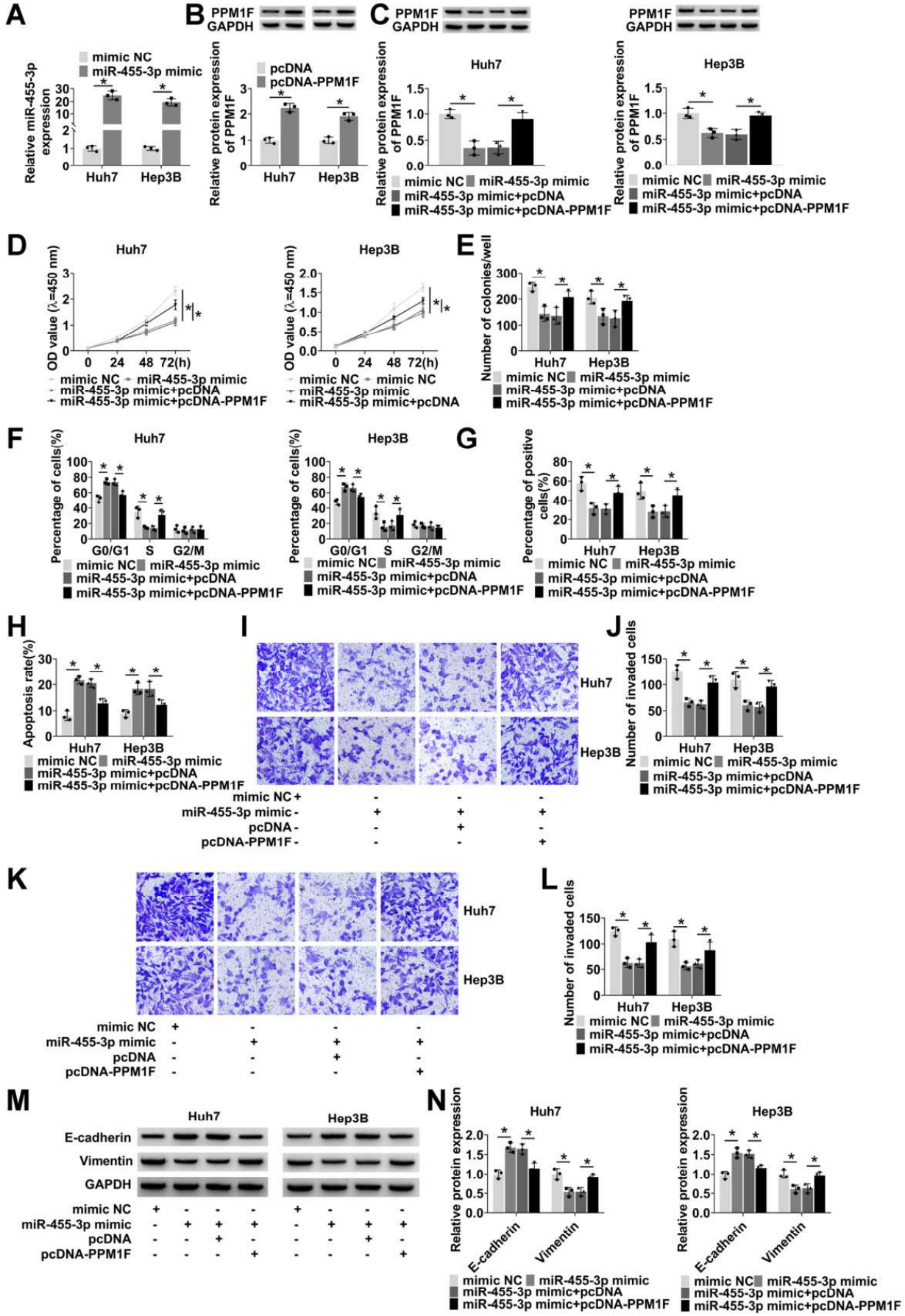

Fig. 7 Download full resolution image